International Journal of Science and Research (IJSR)
ISSN (Online): 2319-7064
Index Copernicus Value (2013): 6.14 | Impact Factor (2013): 4.438

Transient Stability Analysis of SMIB in Power System Using Artificial Neural Network

Sanoj Kumar[1], Girish Dalal[2]

[1]Post Graduate, Student at Mewar University, Rajasthan, India

[2]Assistant Professor in EE Dept., Mewar University, Rajasthan, India

Abstract: ***In this paper, a Neural network based PSS is proposed to control the low-frequency oscillation present in single machine infinite bus system (SMIB). The Neuro-PSS consists of two neural networks: Neuro-Identifier, which emulates the characteristics of power flow and Neuro-Controller, which produce supplementary excitation signal. Proposed PSS helps in improving stability-constrained operating limits in large generators. The action of proposed PSS is to provide damping to the oscillations of the synchronous machine rotor through generator excitation. This damping is provided by an electric torque applied to the rotor that is in phase with speed variation Δω, which is feedback input signal to proposed PSS. The control objective is Quadratic function applied by neuro-controller over outputs produced by system plant and neuro- identifier.***

Keyword: PSS, Oscillation, ANN, Neuro-Identifier.

1.Introduction

DESIGN and application of power system stabilizers (PSS) has been the subject of continuing development for many years. The conventional PSS (CPSS) is an analog or digital implementation of lead–lag networks. Many investigators have treated power system stabilizer design as an eigen structure assignment or pole placement [1]–[5]. This involves obtaining a frequency response of the systems.

1.1 Low Frequency Oscillation

Low frequency oscillations (LFO) are generator rotor angle oscillations having a frequency between 0.1 -2.0 Hz and are classified based on the source of the oscillation. The LFO can be classified as:

1.1.1 Intra plant Oscillations

Intra plant oscillations are confined within a plant when generators oscillate against each other. The frequency of oscillations in this mode is generally in the range of 2-3 Hz. This is not very common and PSS is not designed to cope with this mode.

1.1.2 Local Mode Oscillations

The frequency of oscillation in this mode is generally in the range of 1-2 Hz. Experience has shown that these oscillations tend to occur when a very weak transmission line exists between a station and its load centre or when units are required to operate at high steady state power angles between the generator internal voltage and the infinite bus voltage.

1.1.3 Inter-Area Mode Oscillations

Inter area oscillations involve combinations of many machines on one part of a system swinging against machines on another part of the system. The characteristic frequency of inter area oscillation is generally in range of 0.1-0.6 Hz. It is lower than local mode frequencies because of higher effective reactance of the tie lines between these large systems. It is recognized that the normal action of voltage regulators on generating units has the potential of introducing negative damping in the excitation control system. This may result in undamped modes of oscillations.

2. System Modeling

To study the control of power system oscillations, single-machine system connected to infinite bus (SMIB) through a transmission line, is taken. The SMIB consists of a synchronous generator, a turbine, a governor, an excitation system and a transmission line connected to an infinite bus. The mathematical model for all the elements of the system is developed using the Heffron-Phillips model. The model is built in MATLAB/SIMULINK environment.

2.1 Modelling of Synchronous Machine

In developing equations of a synchronous machine, the following assumptions are made [4].The stator windings are sinusoidal distributed along the air-gap as far as the mutual effects with the rotor are concerned.

a) The stator slots cause no appreciable variation of the rotor inductances with rotor position.
b) Magnetic hysteresis is negligible.
c) Magnetic saturation effects are negligible.

Assumptions (a),(b) and (c) are reasonable, while (d) is made for the convenience of analysis. The machine equations will be developed first by assuming linear flux-current relationships [4].

Fig.1 shows the circuits involved in the analysis of a synchronous machine. The stator circuits consist of three-phase armature windings carrying alternating currents. The rotor circuit comprises field and amortisseur (or damping) windings. The field winding is connected to a source of direct current. The current in amortisseur may be considered to flow in two sets of closed circuits: one set whose flux is in line with that of the field along the d-axis and another set whose flux is at right angles to the field axis or along the q-axis.

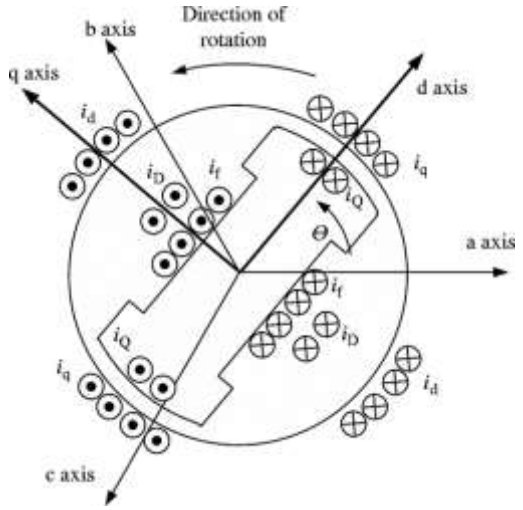

Figure 2.1: Synchronous Machine Diagram

2.1.1 Stator circuit equations

The voltage equations of three phases are:

$$e_a = \frac{d\psi_a}{dt} - R_a i_a = p\psi_a - R_a i_a \quad (2.1)$$

$$e_b = \frac{d\psi_b}{dt} - R_a i_b = p\psi_b - R_a i_b \quad (2.2)$$

$$e_a = \frac{d\psi_c}{dt} - R_a i_a = p\psi_c - R_a i_c \quad (2.3)$$

The flux linkage in the phase a winding at any time is given by

$$\psi_a = -l_{aa} i_a - l_{ab} i_b - l_{ac} i_c + l_{afd} i_{fd} + l_{akd} i_{kd} + l_{akq} i_{kq} \quad (2.4)$$

Similar expressions apply to flux linkages of windings b and c.

2.1.2 Rotor circuit equations

The rotor circuit voltage equations are:

$$e_{fd} = p\psi_{fd} - R_{fd} i_{fd} \quad (2.5)$$

$$0 = p\psi_{kd} - R_{kd} i_{kd} \quad (2.6)$$

$$0 = p\psi_{kq} - R_{kq} i_{kd} \quad (2.7)$$

The rotor circuit flux linkages may be expressed as follows:

$$\psi_{fd} = L_{ffd} i_{fd} + L_{fkd} i_{kd} - L_{afd}[i_a \cos\Theta + i_b \cos(\Theta - 2\pi 3 + i_c \cos\theta + 2\pi 3] \quad (2.8)$$

$$\psi_{kd} = L_{fkd} i_{fd} + L_{kkd} i_{kd} - L_{akd}[i_a \cos\Theta + i_b \cos\left(\Theta - \frac{2\pi}{3}\right) + i_c \cos\left(\theta + \frac{2\pi}{3}\right)] \quad (2.9)$$

$$\psi_{kq} = L_{kkq} i_{kq} + L_{akq}[i_a \sin\Theta + i_b \sin\left(\Theta - \frac{2\pi}{3}\right) + i_c \sin\left(\theta + \frac{2\pi}{3}\right)] \quad (2.10)$$

3.dq0 Transformation

Direct axis is aligned with the rotor's pole. Quadrature axis refers to the axis whose electrical angle is orthogonal to the electric angle of direct axis.

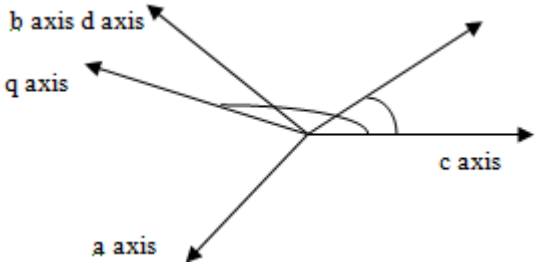

Figure 3.1: dq- axis.

Stator quantities (S_{abc}) of current, voltage and flux can be converted to the quantities (S_{dqo}) referenced to the rotor. This conversion comes through K matrix.

$$S_{dqo} = K\, S_{abc} \quad (2.11)$$

$$S_{abc} = K^{-1} S_d \quad (2.12)$$

Where

$$K = \frac{2}{3}\begin{bmatrix} \cos(\theta_{me}) & \cos(\theta_{me} - \frac{2\pi}{3}) & \cos(\theta_{me} + \frac{2\pi}{3}) \\ -\sin(\theta_{me}) & -\sin(\theta_{me} - \frac{2\pi}{3}) & -\sin(\theta_{me} + \frac{2\pi}{3}) \\ \frac{1}{2} & \frac{1}{2} & \frac{1}{2} \end{bmatrix} \quad (2.13)$$

$$K^{-1} = \begin{bmatrix} \cos(\theta_{me}) & -\sin(\theta_{me}) & 1 \\ \cos(\theta_{me} - \frac{2\pi}{3}) & -\sin(\theta_{me} - \frac{2\pi}{3}) & 1 \\ \cos(\theta_{me} + \frac{2\pi}{3}) & -\sin(\theta_{me} + \frac{2\pi}{3}) & 1 \end{bmatrix} \quad (2.14)$$

3.2.1 Stator Voltage Equation in dqo Components

Eq.2.1 to 2.3 is basic equations for phase voltages in terms of phase flux linkages and currents. By applying the dqo transformation of equation 2.11, the following expression in terms of transformed components of voltage, flux linkages and currents result:

$$e_d' = p'\psi_d' - \psi_q'\omega_r' - R_a' i_d' \quad (2.15)$$

$$e_q = p\psi_q + \psi_d p\theta - R_a i_q \quad (2.16)$$

$$e_o = p\psi_o - R_a i_o \quad (2.17)$$

The angle θ, as defined in Fig. 1.1, is the angle between the axis of phase a and d-axis. The term pθ in the above equations represents the angular velocity ω_r of the rotor. With time in per unit equation 2.15 to 2.18 can be written as:

$$e_d' = p'\psi_d' - \psi_q'\omega_r' - R_a' i_d' \quad (2.18)$$

$$e_d' = p'\psi_q' - \psi_d'\omega_r' - R_a' i_q' \quad (2.19)$$

$$e_d' = p'\psi_o' - R_a' i_o' \quad (2.20)$$

The per unit derivative appearing in the above equations is given by:

$$p' = \frac{d}{dt'} = \frac{1}{\omega_{base}} \cdot \frac{d}{dt} = \frac{1}{\omega_{base}} p \quad (2.21)$$

3.2.3 Per Unit Rotor Voltage Equation

From equation 2.5 to 2.7, we can obtain per unit field voltage equation:

$$e_{fd}' = p'\psi_{fd}' + R_{fd}' i_{fd}' \quad (2.22)$$

$$0 = p'\psi_{kd}' + R_{kd}' i_{kd}' \quad (2.23)$$

$$0 = p'\psi_{kq}' + R_{kq}' i_{kq}' \quad (2.24)$$

3.4 Dynamics of SMIB System

The single machine connected to infinite bus through an external reactance X_{eff} and resistance R_e is widely used configuration and armature resistance is equal to zero [7]. Figure 2.3 shows the SMIB system without controller.

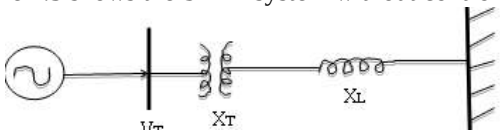

Figure 3.2: Single Machine Connected to Infinite bus.

$$E'_q + X'_d i_d = V_q \quad (2.25)$$

$$-X_q i_q = V_q \quad (2.26)$$

The complex terminal voltage can be expressed as:

$$V_Q + jV_D = (V_q + jV_d)e^{i\delta} = (i^q + ji_d)(R_e + jX_{eff})e^{i\delta} + V_B < 0 \quad (2.27)$$

which is given as:

$$(V_q + jV_d) = (i^q + ji_d)(R_e + jX_{eff}) + V_B e^{-i\delta} \quad (2.28)$$

Separating real and imaginary parts, equation (2.28) can be express as

$$V_q = R_e i_q - X_{eff} i_d + V_B \cos\delta \quad (2.29)$$

$$V_q = R_e i_d - X_{eff} i_d + V_B \sin\delta \quad (2.30)$$

Substituting equation (2.29) and (2.30) in equation (2.25) and (2.26), we get

$$\begin{bmatrix} X'_d & -R_e \\ -R_e & -(X_q + X_{eff}) \end{bmatrix} \begin{bmatrix} i_d \\ i_q \end{bmatrix} = \begin{bmatrix} V_B \cos\delta - E'_q \\ -V_B \sin\delta \end{bmatrix} \quad (2.31)$$

The expression for i_d and i_q are obtained from solving equation (2.31) and are given below:

$$i_d = \frac{1}{A}[R_e V_B \sin\delta + (X_q + X_{eff})(V_B \cos\delta - E'_q)] \quad (2.32)$$

$$i_q = \frac{1}{A}[(X'_d + X_{eff})V_B \sin\delta - R_e(V_B \cos\delta - E'_q)] \quad (2.33)$$

Where

$$A = (X'_d + X_{eff})(X_q + X_{eff}) + R_e^2 \quad (2.34)$$

Linearizing equations (2.32) and (2.33) we get:

$$\Delta i_d - = C_1 \Delta\delta + C_2 E'_q \quad (3.35)$$

$$\Delta i_q - = C_3 \Delta\delta + C_4 E'_q \quad (2.36)$$

Where

$$C_1 = \frac{1}{A}[R_e V_B \cos\delta_0 - (X_q + X_{eff})V_B \sin\delta_0] \quad (2.37)$$

$$C_2 = -\frac{1}{A}(X_q + X_{eff}) \quad (2.38)$$

$$C_3 = \frac{1}{A}[(X_d + X_{eff})V_B \cos\delta_0 + R_e V_B \sin\delta_0] \quad (2.39)$$

$$C_4 = \frac{R_e}{A} \quad (2.40)$$

Linearizing equation (2.25) and (2.26), and then substituting from equation(2.35) and (2.36), we get

$$\Delta V_q = X'_d C_1 \Delta\delta + (1 + X'_d C_2)\Delta E'_q \quad (2.41)$$

$$\Delta V_d = -X_q C_3 \Delta\delta - X_q C_4 \Delta E'_q \quad (2.42)$$

It is to be noted that here the subscript 'o' indicates operating value of the variable.

3.4.1 ROTOR MECHANICAL EQUATIONS AND TORQUE ANGLE LOOP

The rotor mechanical equations are:

$$\frac{d\delta}{dt} = \omega_B(S_m - S_{mo}) \quad (2.43)$$

$$2H\frac{dS_m}{dt} = D(S_m - S_{mo}) + T_m - T_e \quad (2.44)$$

$$T_e = E'_q i_q + (X'_d - X'_q) i_d i_q \quad (2.45)$$

Linearizing equation (2.45), we get

$$\Delta T_e = [E'_{qo} - (X_q - X'_d) i_{do}]\Delta i_q + i_{qo}\Delta E'_q - (X_q - X'_d) i_{qo}\Delta i_d \quad (2.46)$$

Substituting equation (2.35) and (2.36), we can express as:

$$\Delta T_e = K_1 \Delta\delta + K_2 \Delta E'_q \quad (2.47)$$

Where:

$$K_1 = E_{qo} C_3 - (X_q - X'_d) i_{qo} C_1 \quad (2.48)$$

$$K_2 = E_{qo} C_4 + i_{qo} - (X_q - X'_d) i_{qo} C_1 \quad (2.49)$$

$$E_{qo} = E'_{qo} - (X_q - X'_d) i_{do} \quad (2.50)$$

Linearizing equations (2.43) and (2.44), and applying Laplace transform, we get

$$\frac{d\delta}{dt} = \frac{\omega_B}{s}\Delta S_m \quad (2.51)$$

$$\Delta S_m = \frac{1}{2Hs}[\Delta T_m - \Delta T_e - D\Delta S_m] \quad (2.52)$$

The combined equations (2.47), (2.51) and (2.52) represent a block diagram shown in Figure 3 .4.

3.4.2 Representation of Flux Decay

The equation for field winding can be expressed as:

$$T'_{do}\frac{dE'_q}{dt} = E_{fd} - E'_q + (X_d - X_q) i_d \quad (2.53)$$

Linearizing equation (2.53) and substituting from equation (2.35) we have

$$T'_{do}\frac{d\Delta E'_q}{dt} = \Delta E_{fd} - \Delta E'_q + (X_d - X'_d)(C_1\Delta\delta + C_2\Delta E'_q) \quad (2.54)$$

Taking Laplace transform of (2.54), we get

$$(1 + sT'_{do}K_3)\Delta E'_q = K_3\Delta E_{fd} - K_3K_4\Delta\delta \quad (2.55)$$

Where

$$K_3 = \frac{1}{[1-(X_d - X'_d)C_2]} \quad (2.56)$$

$$K_4 = -(K_d - K'_d)C_1 \quad (2.57)$$

Equation (2.55) can be represented by the block diagram .

3.4.3 Representation of Excitation System Model

The inputs to the excitation system are the terminal voltage V_T, reference voltage V_R [9]. , K_A and T_A represents the gain and time constant of the excitation system [6].It can expressed as

$$\Delta V_t = \frac{V_{do}}{V_{to}}\Delta V_d + \frac{V_{qo}}{V_{to}}\Delta V_q \quad (2.58)$$

Substituting from equations (2.41) and (2.42), we get

$$\Delta V_t = K_5\Delta\delta + K_6\Delta E'_q \quad (2.59)$$

Where

$$K_5 = \left(\frac{V_{do}}{V_{to}}\right)X_q C_3 + \left(\frac{V_{qo}}{V_{to}}\right)X'_d C_1 \quad (2.60)$$

$$K_6 = -\left(\frac{V_{do}}{V_{to}}\right)X_q C_4 + \left(\frac{V_{qo}}{V_{to}}\right)(1 + X'_d C_2) \quad (2.61)$$

4.1 Overall System Representation

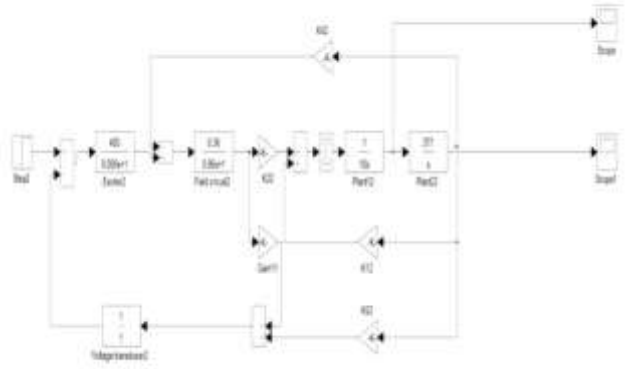

Figure 4.1: Block Diagram representation of the system

4.2 System Representation with Conventional PSS

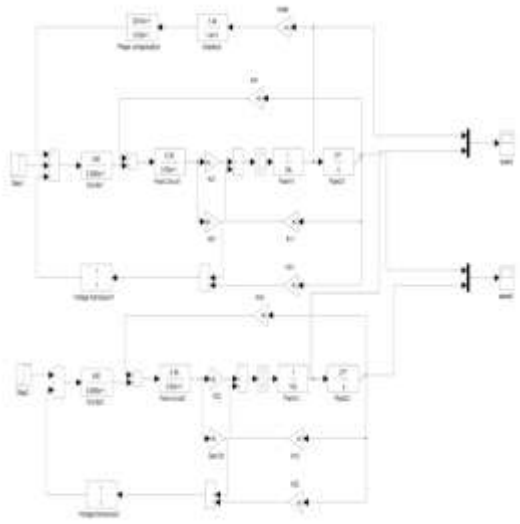

Figure 4.2: Block Diagram representation of System with the Conventional PSS

4.4 Simulation Results Comparing NN-PSS with Conventional PSS

CASE 1: For the Low loading condition: P = 0.4 and Q = 0.7 (in p.u.)

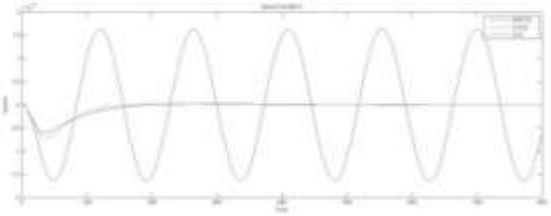

Figure 4.1: Speed Deviation for ANN-PSS and Conventional PSS

Figure 4.1 shows Speed deviation for Neural network based PSS (NNPSS) and Conventional PSS (CPSS) against time. The first peak value for NNPSS is -0.0005 at 0.105 sec and for CPSS it is -0.0007 at 0.16 sec.

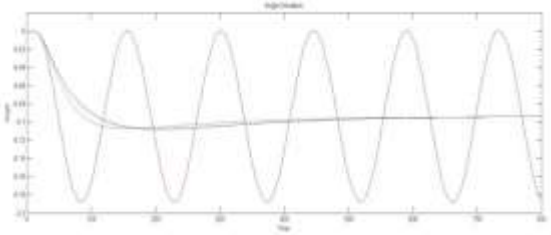

Figure 4.2: Angle Deviation for ANN-PSS and Conventional PSS

Figure 4.2 shows Angle deviation for NNPSS and CPSS against time. The first peak value for NNPSS is -0.1102 at 1.8 second for CPSS it is -0.1.72 at 0.9 sec.

4.Conclusion

The results of proposed NN-PSS is compared with the conventional PSS over a SMIB system. The performance of NN-PSS is satisfactory and is able to damp the low-frequency oscillation in the system.

References

[1] László Z. Rác and Béla Bókay, "Power System Stability", Akadémiai Kiadó, Budapest, 1988.
[2] Grahan Rogers "Demystifying power system oscillations", IEEE Computer Application in Power, Vol. 9, No. 3, pp 30-35, July 1996.
[3] Y. N. Yu, "Electric power system dynamics", Academic press 1983.
[4] F. P. DeMello and C. A. Concordia, "Concept of synchronous machine stability as affected by excitation control", *IEEE Trans. On PAS*, Vol. PAS-103, pp. 316-319, 1969.
[5] F. P. demello and T. F. Laskowaski, "Concept of Power System Dynamic Stability", IEEE Trans. PAS, Vol.94, pp.827-833, 1975.
[6] I. Ngamroo and S. Dechanupaprihta, "Design of Robust H_∞ Power System Stabilizer using Normalized Coprime Factorization", AJSTD, Vol,19, Issue 2, pp.85-96, August 2002.
[7] M. R. Khalidi, A. K. Sarkar, K. Y. Lee, Y. M. Park, "The model performance measure for parameter optimization of power system stabilizer", IEEE Trans EC, Vol. 8, Dec. 1993.

Author Profile

Sanoj Kumar received the Bachelor of technology degrees in Electrical and Electronics Engineering from MDU, Rohtak in 2011 and currently pursuing M. tech Degree from Mewar University.His research interests including power system stability and control,restructure of power system,optimization and control.

Girish Dalal received the M.TECH Degree at DAVV(IET) INDORE from instrumentation engg.in 2010.Currently working as Assistant Prof.in EE Dept. in Mewar university. His research interested in instrumentation, power system transient stability, protection and facts devices.